energies

MDPI

Article

Effects Generated by the Magnetic Core Anisotropy of an Induction Motor

Adam Warzecha * and Witold Mazgaj

Institute of Electromechanical Energy Conversion, Cracow University of Technology, 31-155 Kraków, Poland; pemazgaj@cyfronet.pl

* Correspondence: adam.warzecha@pk.edu.pl

Received: 31 March 2020; Accepted: 21 April 2020; Published: 30 April 2020

Abstract: A theoretical analysis enables effects generated by the magnetic core anisotropy of an induction motor to be determined qualitatively. Relationships formulated between currents and magnetic flux linkages that are associated with three-phase stator windings enable the qualitative determination of spectra of currents or voltages of a typical induction motor. These relationships account for nonlinear and anisotropic magnetization characteristics of the motor core, both during idle running and motor starting. Based on these relationships, components of the amplitude Fourier spectra of symmetrical components of currents or voltages, which are useful in the diagnostics of stator or rotor core anisotropy, were selected. Field calculations were performed for the core of a two-pole 5.5 kW motor supplied by three-phase sinusoidal currents. The components of the induced voltage Fourier spectra in both the idle running and short-circuit state were similar to analogous components predicted based on theoretical studies. The components occurring in the spectra, which were obtained based on field calculations, were distinguished in the measured spectra of the symmetrical components of the phase currents. These components were applied to estimate representative current signal levels in the diagnostics of motor core anisotropy. Relative values of these signals did not exceed 60 dB; however, they were significant for assessing the internal asymmetry level of the motor stator or rotor core. The results of laboratory measurements confirmed the results of the theoretical analysis.

Keywords: induction motor; magnetic anisotropy; frequency analysis; diagnostics; motor current analysis

1. Introduction

Magnetic cores of electrical rotating motors are constructed using non-oriented steel sheets which should have isotropic properties; however, these sheets have certain anisotropy [1,2]. The anisotropy of the magnetic cores causes fluctuations of the magnetic rotating field in the rotating motors. This phenomenon can be especially noticed in two-pole induction motors, which are distinguished by a short path of the magnetic flux in the air gap. The saturation level of the teeth and yokes of the magnetic core has a significant influence on the amplitudes of these fluctuations [3]. The fluctuations of the rotating field cause disturbances in phase currents and voltages induced in stator windings, which result in parasitic components in the electromagnetic torque. Currently, these phenomena are considered in the design of electrical drive control systems [4,5]; model studies using Finite Elements Analysis techniques can predict and explain these phenomena [6–9]. The fluctuation of the co-energy of the rotating magnetic field can be treated as a good indicator for the anisotropy of both the stator and the rotor. This conclusion was confirmed by field calculations performed for a medium-sized squirrel cage induction motor. In order to do that, a circuit model of this motor with an anisotropic core was prepared, assuming that the magnetic flux density along the air gap has a sinusoidal distribution.

The circuit model is based on properties of the co-energy function of the magnetic field excited by winding currents. This function has a simple form when the equivalent magnetising current is used and magnetic leakage fields are described separately. This enabled mathematical formulas to be simplified in cases where nonlinear magnetisation characteristics should be considered. The unambiguous magnetisation characteristics of the non-oriented sheets were determined on the basis of magnetic hysteresis loops measured for the direction of both the easy and hard magnetisation [10]. In the above-mentioned model, the common features of relations concerning flux linkages and currents are a consequence of using the prime co-energy function of the main field as the function of the magnetising current. These relations depend on the magnetomotive (MMF) axis position. They can model a non-zero angle between the MMF axis and the flux density field axis. In this approach, the model of the induction motor with the anisotropic core is similar to the model of a two-pole motor with the salient poles of the rotor or the stator [11]. It was applied in the formulation of the proposed circuital model of the induction motor.

The anisotropic properties of the rotor core also affected the leakage fluxes of the stator windings, which refer to parts of leakage fluxes that close through the air gap and rotor teeth. This effect may be evident in starting states, especially when induction motors are supplied by voltage source inverters [5]. The study of these effects may be useful in the diagnostics of motor core quality [12,13] and in the assessments of the internal motor imbalance [14,15].

2. Flux Linkages—Currents Relations in Motors with an Anisotropic Rotor

The co-energy of the magnetic field in the core and in the air gap of the two-pole induction motor with an anisotropic rotor core is a function of N independent currents i_n of the windings and the angular position ϕ of the rotor. In the circuit model of the rotating motors the main circuit and leakage magnetic circuits are described separately. This is also acceptable when the nonlinear magnetising characteristic of the core is taken into account due to the specified magnetic circuits being saturated under different conditions. Therefore, the global field co-energy can be expressed as a sum of the main field co-energy and the co-energies of the leakage fields:

$$E(i_1, \ldots, i_N, \varphi) \approx E_\mu\left(i_\mu, \alpha_\mu, \varphi\right) + \sum_{n=1}^{N} E_{\sigma_n}(i_n, \varphi) \tag{1}$$

The main co-energy function can be written as a function of only three equivalent variables: the magnetizing current i_μ, which corresponds to the amplitude of the fundamental harmonic of the total MMF; the angular position α_μ of the total MMF axis in the air-gap with respect to the axis of the stator easy magnetization; and the angle of the rotor position ϕ (Figures 1 and 2). The co-energies of the leakage fields depend on the individual winding currents and the angle of the rotor position. The space vector of the rotating magnetizing current is specified in a complex domain by the following formula:

$$\hat{i}_\mu = \frac{2}{\pi} \sum_{n=1}^{N} \nu_n^{(1)} \cdot i_n \cdot e^{j\alpha_n} \tag{2}$$

where N denotes the number of independent stator and rotor currents, the angle α_n is an angular position of the nth winding magnetic axis versus the stator axis or the rolling direction (RD) rotor axis, and $\nu_n^{(1)}$ denotes the winding coefficient for the fundamental spatial harmonic of the flux density distribution in the air gap. Therefore, the absolute value and the argument of the magnetizing current can be written as follows:

$$i_\mu = \mathrm{abs}\left(\hat{i}_\mu\right) \quad \alpha_\mu = \arg\left(\hat{i}_\mu\right) \tag{3}$$

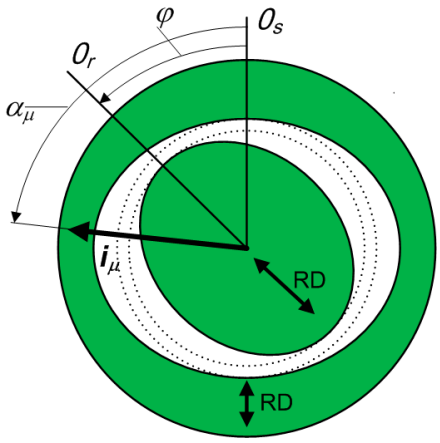

Figure 1. Representation of the induction motor core with anisotropic features modelled by a non-uniform air gap; RD denotes the direction of the easy magnetization axis of the stator and rotor core; dotted lines indicate the air gap for a motor without anisotropy; and 0_s, 0_r denote axes of the stator and rotor, respectively.

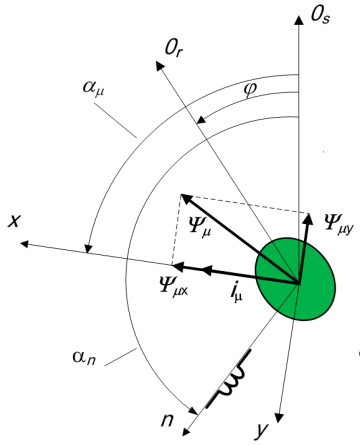

Figure 2. Variables of the mathematical description of the nonlinear and anisotropic motor core; the coil represents the nth independent winding.

An approximation using the complex Fourier series is proposed to write separately the independent angular variables:

$$E_\mu\left(i_\mu, \alpha_\mu, \varphi\right) = \sum_k \sum_l E_{\mu_{k,l}}\left(i_\mu\right) \cdot e^{jk\alpha_\mu} \cdot e^{jl\,(\alpha_\mu - \varphi)} \tag{4}$$

The double series (4) express the main co-energy function in dependence on the position of the magnetising current vector versus the stator and rotor RD axis. For a three-phase squirrel cage induction motor with a uniform air gap and a linear isotropic magnetic core: $k = l = 0$. For a nonlinear and anisotropic core where $k, l = \{0, \pm 2, \pm 4, \dots\}$, the co-energies of the stator leakage fields can be approximated using a similar complex Fourier series:

$$E_{\sigma_n}(i_n, \varphi) = \sum_l E_{\sigma_{n,l}}(i_n) \cdot e^{j2l(\varphi - \alpha_n)} \tag{5}$$

The independent winding flux linkages are defined as the partial derivatives of the co-energy function with respect to the independent currents:

$$\psi_n = \frac{\partial E}{\partial i_n} = \frac{\partial E_\mu}{\partial i_n} + \frac{\partial E_{\sigma_n}}{\partial i_n} = \psi_{\mu_n} + \psi_{\sigma_n} \tag{6}$$

The main flux linkage of each separate winding can be written as follows:

$$\psi_{\mu_n} = \frac{\partial E_\mu}{\partial i_\mu}\frac{\partial i_\mu}{\partial i_n} + \frac{\partial E_\mu}{\partial \alpha_\mu}\frac{\partial \alpha_\mu}{\partial i_n} \tag{7}$$

Hence, the result of the differentiation operations above can be written as follows:

$$\psi_{\mu_n} = \psi_{\mu_x} v_n^1 \cos\left(\alpha_n - \alpha_\mu\right) + \psi_{\mu_y} v_n^1 \sin\left(\alpha_n - \alpha_\mu\right) \tag{8}$$

Subsequently, the main flux linkage of each separate winding can be expressed using two components: component 'x' in the direction of the magnetizing current spatial vector and component 'y' in the perpendicular axis (Figure 2). The amplitudes of these components are expressed by the following series:

$$\psi_{\mu_x}\left(i_\mu, \alpha_\mu, \varphi\right) = \sum_k \sum_l \psi_{\mu_{x,k,l}}\left(i_\mu\right) \cdot e^{j[(k+l)\alpha_\mu - l\varphi]} \tag{9}$$

$$\psi_{\mu_y}\left(i_\mu, \alpha_\mu, \varphi\right) = \sum_k \sum_l j \cdot (k+l) \cdot \psi_{\mu_{y,k,l}}\left(i_\mu\right) \cdot e^{j[(k+l)\alpha_\mu - l\varphi]} \tag{10}$$

The functional coefficients $\psi_{\mu_{x,k,l}}(i_\mu)$ and $\psi_{\mu_{y,k,l}}(i_\mu)$ of the series are the equivalent internal magnetization characteristics in the perpendicular x and y axes, respectively. They are associated with the elements of the co-energy Fourier series by the following formulas:

$$\psi_{\mu_{x,k,l}} = \frac{\partial E_{\mu_{k,l}}}{\partial i_\mu}, \ \psi_{\mu_{y,k,l}} = \frac{E_{\mu_{k,l}}}{i_\mu} \tag{11}$$

Based on Equations (7)–(9), the series that approximates the main flux linkage of each nth independent circuit can be written in the following complex form:

$$\psi_{\mu_n} = \frac{1}{2} v_n^1 \sum_m \sum_k \sum_l \left(\psi_{\mu_{x,k,l}} + (k+l) \cdot m \cdot \psi_{\mu_{y,k,l}}\right) \cdot e^{j\delta_{n,m,k,l}} \tag{12}$$

where

$$\delta_{n,m,k,l} = (k + l - m) \cdot \alpha_\mu - l\varphi + m\alpha_n \qquad \text{for } m = \{-1, \ 1\}. \tag{13}$$

Owing to the nonlinearity of the main magnetic circuit, the third harmonic of the flux density distribution along the air gap generates a significant component of the main flux linkages. Hence, the formula approximating the main flux linkages of the stator winding should be completed by the following component:

$$\psi_{\mu_n}^{(3)} = \frac{1}{2} v_n^{(3)} \sum_m \psi_\mu^{(3)}\left(i_\mu\right) e^{j3m(\alpha_n - \alpha_\mu)} \tag{14}$$

where the constant $v_n^{(3)}$ denotes the winding coefficient of the third harmonic.

The leakage fluxes of the stator windings can be approximated by Series (15), considering both the core anisotropy in the linear magnetic condition and the effect of the rotor slots:

$$\psi_{\sigma_n} = \left(\sum_l L_{\sigma_{n,l}} \cdot e^{j \cdot l(\varphi - \alpha_n)}\right) \cdot i_n \tag{15}$$

where $L_{\sigma_{n,l}}$ denotes the coefficients of the series approximating the leakage inductance versus rotor position.

Formulas (12), (14), and (15) enable the frequency components of the voltage Fourier spectra caused by the motor core anisotropy to be determined.

3. Predicted Spectra of Induced Stator Phase Voltages

The magnetising current defined by formula (3) has a constant value when the motor operates in a steady-state; however, the angular positions of both the magnetising current space vector (2) and the rotor change linearly with time:

$$i_\mu = const., \quad \alpha_\mu = \omega_0 t + \alpha_0, \quad \varphi = (1-s)\cdot\omega_0 t + \varphi_0 \tag{16}$$

where ω_0 is the fundamental pulsation and s denotes the rotor slip.

Substituting variables α_μ, φ in Equation (13) and in Series (15) by the assumed time functions (16), the pulsation of the predicted components of the main flux linkages can be specified as follows:

$$\omega_\rho = \rho\cdot\omega_0 = \{(k-m+ls)\cdot\omega_0 \quad \cup \quad 3m\cdot\omega_0\} \tag{17}$$

where ρ denotes multiples of the fundamental pulsation.

The fundamental component was expressed for $k = l = 0$ resulting in $\rho = \pm 1$. The higher significant components were obtained for abs(k) + abs(l) ≤ 4. When only the stator core was magnetically anisotropic, the flux linkage pulsation components were indicated for $k \neq 0$ and $l = 0$, resulting in $\rho = (\pm 1, \pm 3, \pm 5)$. Meanwhile, when the rotor core was magnetically anisotropic, the flux linkage components were indicated for $k = 0$ and $l \neq 0$, resulting in $\rho = \pm(1 \pm 2s)$, $\pm(1 \pm 4s)$, ... When both the stator and the rotor core were magnetically anisotropic, the additional components of the series shown in (12) and (15) obtained for $k = l = \pm 2$ and $k = -l$ should be considered; therefore, $\rho = \pm(1 \pm 2s)$, $\pm(3 \pm 2s)$, ...

The main phase voltages induced in the three-phase stator windings are time derivatives of the corresponding phase flux linkages according to formula:

$$e_{\mu_n} = \frac{1}{2}\nu_n^{(1)} \sum_m \sum_k \sum_l j\rho\omega_0 \psi_{\mu_{m,k,l}} e^{j\delta_{n,m,k,l}} + \frac{1}{2}\nu_n^{(3)} \psi_\mu^{(3)} \sum_m j3m\omega_0 e^{j3m(\omega_0 t + m\alpha_n)} \tag{18}$$

The Fourier series components of the induced main voltage are the same as those for the main flux linkages. Relative amplitudes of the induced voltage components are equal to those of the flux linkage components multiplied by the corresponding pulsation. The specified series components enable the separation of the positive-, negative-, or zero-sequence symmetrical components of the phase voltage. They can be determined using Formula (19):

$$\delta_{n,m,k,l} = (k-m+ls)\cdot\omega_0 t + m\alpha_n + (k+l-m)\alpha_0 + l\phi_0 \tag{19}$$

Pulsation components of the phase voltage that fulfil the condition sign($k - m + ls$) $\neq$ sign(m) form the positive-sequence components; otherwise, negative components are formed. The components of the zero-sequence of the phase voltages that were induced by the main flux linkages were not generated by the magnetic core anisotropy; however, these components were induced by the nonlinearity of the core magnetization characteristic.

The stator leakage fields induced additional phase voltage components that can be approximated by the following series:

$$\psi_{\sigma_n} = \sum_m \sum_l L_{\sigma_{n,l}} e^{jl((1-s)\omega_0 t + \varphi_0 - \alpha_n)} I_s e^{jm(\omega_0 t + \alpha_0 - \alpha_n)} \tag{20}$$

$$e_{\sigma_n} = \frac{d\psi_{\sigma_n}}{dt} = \sum_m \sum_l j(l+m-ls)\omega_0 L_{\sigma_{n,l}} I_s e^{j[(l+m-ls)\omega_0 t - (m+l)\alpha_n + m\alpha_0 + l\varphi_0]} \tag{21}$$

The presented analysis enables the predicted voltage frequencies to be listed, which can be generated in a symmetrical induction motor with a magnetically anisotropic core supplied by symmetrical mono-harmonic current sources. The final results are presented in Table 1.

Table 1. Predicted frequencies in Fourier spectra of symmetrical voltage components generated by the magnetic core anisotropy.

Type of Anisotropy	Positive Sequence	Negative Sequence	Zero Sequence
Stator core or unwound rotor core at slip s = 1	$\{f_0, 3f_0, 5f_0\}^{(1)}$	$\{f_0, 3f_0, 5f_0\}^{(1)}$	$f_0{}^{(2)}, 3f_0{}^{(3)}$
Rotor core at slip s ≈ 0	$(1 \pm 2s)f_0{}^{(1)}$ $(1 \pm 4s)f_0{}^{(1)}$	-	$(3–2s)\,f_0{}^{(2)}$ $(3–4s)\,f_0{}^{(2)}$
Two-sided at slip s ≈ 0	$(3 \pm 2s)f_0{}^{(1}$	$(1 \pm 2s)f_0{}^{(1)}$	-

These predicted frequencies are caused by

1. the rotating field in the nonlinear anisotropic core,
2. the leakage stator fields in the anisotropic core,
3. the rotating field in the nonlinear isotropic core.

4. Field Calculations of Effects Generated by an Anisotropic Motor Core

A qualitative and quantitative identification of the magnetic field co-energy, electromagnetic torque, and flux linkages of the stator winding was performed for a 5.5 kW, 400 V, 50 Hz two-pole induction motor (six slots per pole and phase), omitting rotor cage bars. Figure 3 presents a cross-section of the motor core. The magnetic field distribution was calculated assuming that the rotor core was anisotropic and the magnetic permeability in the RD axis was twice as high as in the TD axis, while the stator core and the shaft were isotropic. The axis of the MMF produced by stator currents was parallel to the y axis.

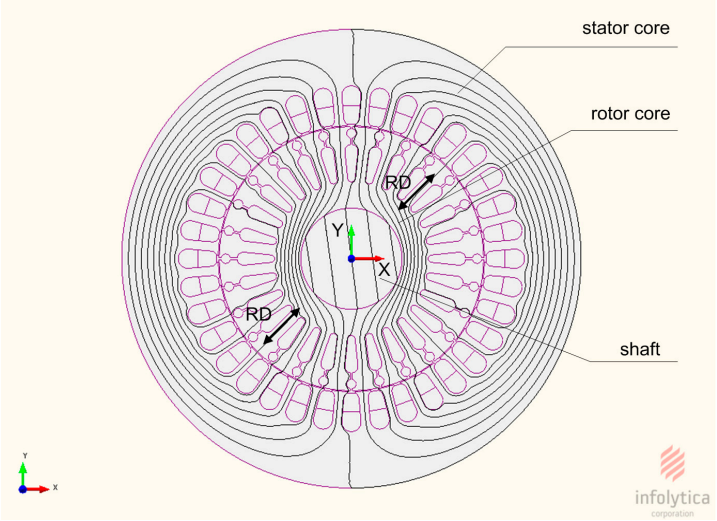

Figure 3. Cross-section of the induction motor core and an example of magnetic field distribution generated by symmetrical currents of the stator for the marked RD axis of the anisotropic rotor.

The unambiguous magnetisation characteristics of the core material were determined for the non-oriented sheet M530-50A (Figure 4).

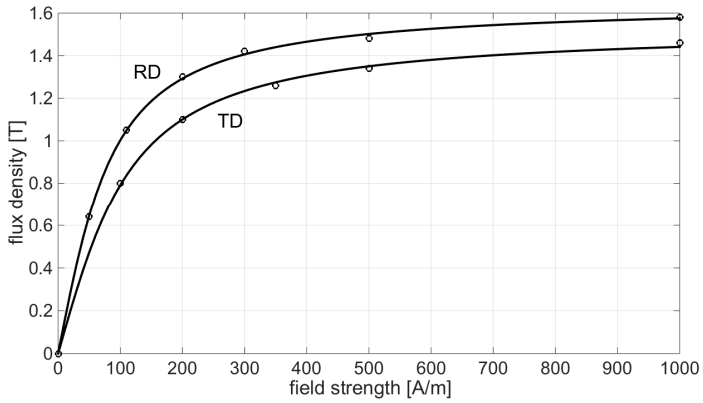

Figure 4. Flux density versus magnetic field strength of dynamo sheet type M530-50A measured along the rolling direction RD and transverse direction TD.

Calculations were performed using MagNet 2D software (Infolytica Corp. Montreal, Canada). Three-phase stator winding was supplied using symmetrical three-phase current sources. The amplitudes of these currents were increased until the flux density in the stator teeth was equal to 1.8 T; the unwound rotor was stationary. The field equation was solved in 200 points in one current period, i.e., in one rotation of the MMF axis in the air gap. The waveforms of the magnetic field co-energy and energy (Figure 5) as well as the flux linkages of the stator phase windings were treated as input values in further analyses. In the next step, the Fourier spectra of these waveforms were calculated. It is noteworthy that for isotropic cores with a sinusoidal distribution of the MMF, the co-energy of the magnetic main field exhibited a constant value. The anisotropic properties of the stator core resulted in even harmonics in the co-energy waveform, which yielded fluctuations in both the electromagnetic torque and flux linkages of the windings.

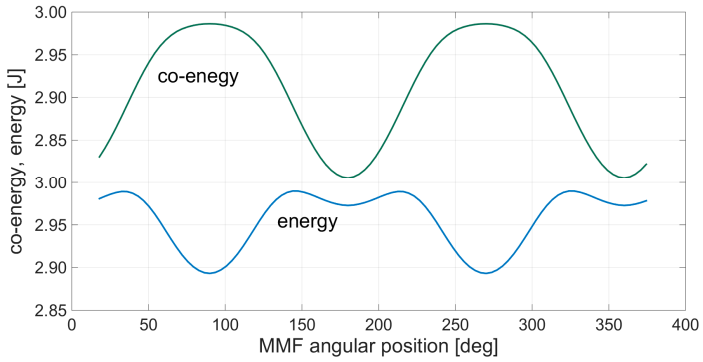

Figure 5. Magnetic field co-energy and energy with respect to the angular position of the stator MMF in the anisotropic stator core for the rated value of the magnetising current.

Similar results were obtained for the anisotropic stator and isotropic rotor. Analogous components occurred in numerical calculations when the same core had two-phase sinusoidal distributed windings. Detailed calculations were performed for the anisotropic rotor core, while the stator core was isotropic. The harmonics of the electromagnetic torque at different values of the magnetising current for the anisotropic rotor core were calculated using the virtual work principle.

The results obtained for relative values of 0.5, 1.0, and 1.5 of the magnetising current (with respect to the rated value 2.7 A) are presented in Table 2.

Table 2. Values of the second and fourth harmonics of the electromagnetic torque generated by the anisotropic stator core for three magnetizing current values.

Parameter	**$2f_0$**			**$4f_0$**		
i_μ (–)	0.5	1.0	1.5	0.5	1.0	1.5
T_e (Nm)	0.01	0.10	0.44	0.01	0.03	0.22

As shown, the amplitudes of the torque harmonics did not exceed 0.1 Nm at the rated magnetizing current, i.e. 1% of the rated torque. It is noteworthy that increasing the magnetizing current from 100% to 150% yielded approximately a 4X increase in the amplitude.

The waveforms of the phase flux linkages, obtained during one turn of MMF axis were examined based on their Fourier spectra. The harmonic components of the flux linkages were used to calculate the symmetrical components individually for each harmonic. Hence, the relative amplitudes of harmonics of the induced phase voltages were calculated using the following formula:

$$U_\rho^r = 20\log\left(\frac{U_\rho}{U_1}10^5\right) \tag{22}$$

where U_1 denotes the fundamental component amplitude.

The harmonics of the symmetrical components of the phase voltages are presented in Table 3.

Table 3. Values of the positive-, negative-, and zero-sequence components of the fundamental, third, and fifth harmonics of the phase voltages for three magnetizing current values.

Parameter	**f_0**			**$3f_0$**			**$5f_0$**		
i_μ (-)	0.5	1.0	1.5	0.5	1.0	1.5	0.5	1.0	1.5
$U_s{}^p$ (dB)	95	100	103	-	43	55	-	43	64
$U_s{}^n$ (dB)	42	50	59	-	58	72	-	-	56
$U_s{}^0$ (dB)	-	-	40	-	-	52	-	-	-

The estimated values of the voltage components were similar to the level of the field calculation accuracy. However, the results were consistent with both the components caused by the core anisotropy and those predicted in Table 1. The negative-sequence component of the third harmonic reached the highest value, i.e., 58 dB at the rated magnetizing current. An increase in the magnetizing current from 100% to 150% yielded an absolute amplitude that was 5x higher (72 dB) than that obtained previously.

The zero-sequence component of the fundamental harmonic (40 dB), as the effect of the anisotropy, was dominated by the zero-component of the third harmonic (52 dB), which was caused by the nonlinearity of the core magnetization characteristic. The results presented in Table 3 indicate the harmonic levels predicted in Table 1 for the motor with an unwound stationary rotor (slip 1). Therefore, the harmonics were generated by the main magnetic field rotating in the motor, and the level of analogical harmonics can be deduced for the motor with a rotor slip of approximately zero.

Additionally, field calculations were performed for cases where the leakage fields dominated over the main field. This refers to the motor operation when the wound rotor rotated with a slip of approximately one. In this case, the model of the motor core was modified by eliminating the main field from the inside the rotor. Furthermore, the leakage fields of the stator can be closed by the anisotropic rotor teeth. Tested effects were obtained when the rotor rotated slowly with respect to the pulsating leakage fields of the stator. Figure 6 shows the spectrum of the zero-sequence components of the phase voltages that were calculated for stator currents with frequency 5 Hz and for the current amplitude that was 3x higher than the rated current; the motor slip was 0.9.

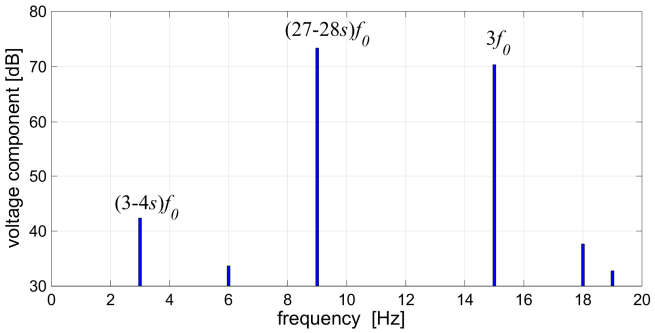

Figure 6. Spectrum of the zero-sequence components of the phase voltages induced only by stator leakage fields when the anisotropy in the rotor teeth was considered; f_0 = 5 Hz and s = 0.9.

The slot harmonic (27–28s) f_0 dominated in the spectrum; however, the harmonic (3–4s) f_0, that was predicted in Table 1 for the anisotropic rotor was evident as well. For the isotropic rotor teeth, the harmonic (3–4s) f_0 did not occur.

It can be expected that harmonics analogous to that indicated in the voltage positive- and negative-sequence component spectra caused by the anisotropy of the core can occur in the stator phase currents when the induction motor is supplied by symmetrical sinusoidal voltage sources. However, the zero-sequence components of the phase currents can occur only for delta-connected windings.

5. Experimental Results

Laboratory experiments were performed to validate conclusions from the analysis of both series that approximated functions of the flux linkages of stator windings and the field calculations. The tested motor, which was supplied directly from a 3 × 400 V grid, operated in idle running at a slip of 0.001. The voltages and phase currents of the stator were saved at a sampling frequency of 10 kS/s; meanwhile, the recording times provided a resolution of at least 0.1 Hz [16]. The magnetic core had a relatively low saturation when the motor was supplied with the rated voltage. Figures 7–10 show results of the motor measurements during idle running. The relative values of the higher harmonics of the currents caused by the anisotropy of the rotor core did not exceed 1% of the fundamental harmonic value. The zero-component of the phase voltages at 50 Hz, which indicates the anisotropy of the stator core, was approximately 43 dB (Figure 7). Additionally, the zero-component of the phase voltages at a frequency of (3–2s)50 Hz = 149.9 Hz and 46 dB (Figure 8) and the positive-sequence components of the phase currents at a frequency of (1 ± 2s)50 Hz = {49.9, 50.1} Hz and above 60 dB (Figure 9) indicated that the rotor core was anisotropic.

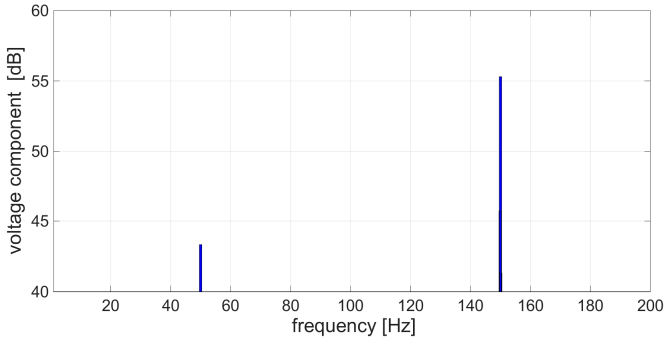

Figure 7. Spectrum of the zero-sequence components of the stator phase voltages in reference to positive component of the voltage fundamental harmonic measured for the tested motor.

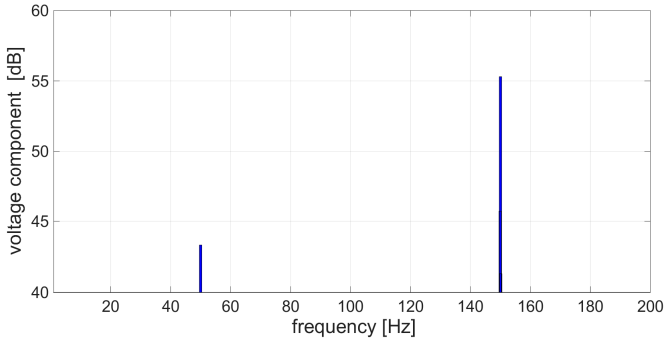

Figure 8. Spectrum details of the voltage zero-sequence component close to the third harmonic.

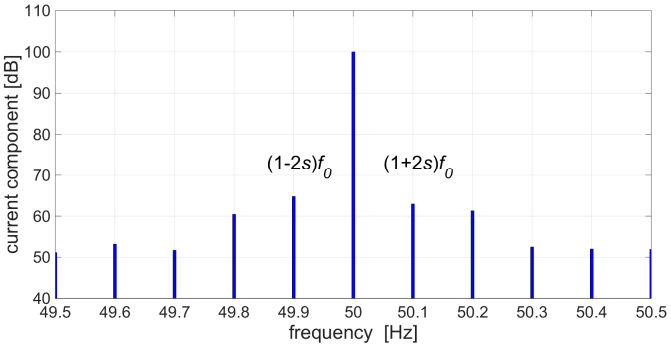

Figure 9. Spectrum of positive-sequence component of the phase currents close to the first harmonic measured for the tested motor.

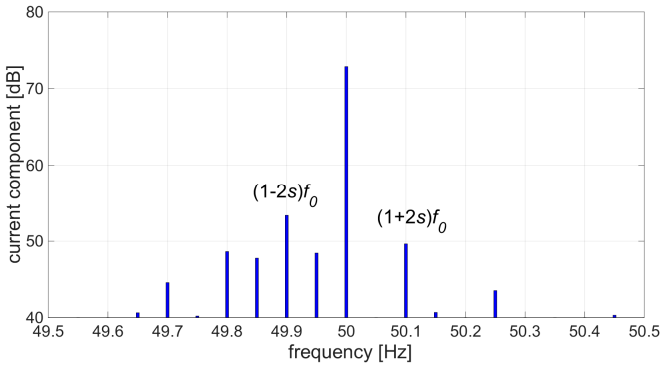

Figure 10. Spectrum of the negative-sequence component of phase currents close to the first harmonic with amplitude ~73 dB in reference to the positive component of the fundamental harmonic measured for the tested motor.

Analogical harmonics at frequency (1 ± 2*s*) 50 Hz = {49.9, 50.1}Hz and values of approximately 50 dB occurred in the spectrum of the negative-sequence component of the phase currents (Figure 10). It is noteworthy that they were predicted as shown in Table 1 for both the stator and rotor core anisotropy.

The results of the measurements allowed us to state that the spectrum of the positive-sequence component of voltages was contaminated, whereas the spectrum of the negative-sequence component had only a fundamental component bigger than 40 dB. It results in the spectrum of the negative-sequence component of phase currents being a more appropriate signal to assess the rotor anisotropy.

6. Conclusions

The anisotropy of the nonlinear magnetization characteristics of the core of the three-phase induction motors contributed to the oscillatory components of both the co-energy and energy of the

rotating magnetic field. Moreover, this anisotropy caused a certain asymmetry of the magnetic leakage fluxes, which resulted in oscillations in the electromagnetic torque. Additionally, modulations of the perimeter of the stator phase current when the motor was supplied by voltage sources or those of the perimeter of the phase voltages when the motor was supplied by current sources were observed. The frequencies of these oscillations in steady states can be determined based on the presented Fourier series that approximate the functions of the winding flux linkages with respect to the position of the rotating field axis.

Similarly, the series that approximates independent phase currents relative to the phase flux linkages can be written based on the functions of the main field energy. These series were formulated with the assumption that the anisotropy can be modelled using the internal magnetization characteristics in both the magnetizing current vector and perpendicular directions. This enabled the dependence between the components of the amplitude spectrum of the voltages and currents and the rotor speed to be determined. The predicted oscillations were separable using field modelling despite their relative values of <1%. A high accuracy of the field calculations was achieved when the windings were supplied by current sources. In this case, only the field equation for the steady states at the rotating spatial vector of the magnetizing current was solved. The amplitude spectra of the induced phase voltages corresponded to the amplitude spectra of the flux linkages of the windings. It is noteworthy that the presentation of the results in the form of the spectra of symmetrical voltage components (field calculations) or in the form of the spectra of symmetrical phase current components (based on measurements) was the most representative for diagnostics purposes. This enabled an analysis of experimental results that were dependent on supply voltage deformations. The frequencies and levels of signals caused by the core anisotropy can be useful in diagnostics pertaining to the asymmetry of motor windings as it generates analogical harmonics of the motor currents.

Author Contributions: Conceptualization, A.W. and W.M.; methodology, A.W.; formal analysis, A.W.; investigation, W.M.; writing—original draft preparation, A.W. and W.M.; writing—review and editing, A.W. and W.M. All authors have read and agreed to the published version of the manuscript.

Funding: This research was funded by the Polish Ministry of Science and Higher Education and performed by the Institute of Electromechanical Energy Conversion (E21, E22) of Cracow University of Technology.

Conflicts of Interest: The authors declare no conflicts of interest.

References

1. Tumański, S. Investigations of the anisotropic behaviour of SiFe steel. *J. Magn. Magn. Mater.* **2003**, *254–255*, 50–53. [CrossRef]
2. Chwastek, K. Anisotropic properties of non-oriented steel sheets. *IET Electr. Power Appl.* **2013**, *7*, 575–579. [CrossRef]
3. Zagradisnik, I.; Hribernik, B. Influence of anisotropy of magnetic material on the saturation harmonics in the three-phase induction motor. *IEEE Trans. Magn.* **1988**, *24*, 491–494. [CrossRef]
4. Wolbank, T.M.; Machl, J.L.; Hauser, H.; Macheiner, P. Lamination Material Anisotropy and Its Influence on the Operation of Inverter-Fed Induction Machines. *IEEE Trans. Magn.* **2003**, *39*, 3283–3285. [CrossRef]
5. Holtz, J.; Hangwen, P. Acquisition of Rotor Anisotropy Signals in Sensorless Position Control Systems. *IEEE Trans. Ind. Appl.* **2004**, *40*, 1379–1397. [CrossRef]
6. Gomez, E.; Roger-Folch, J.; Molina, A.; Fuentes, J.A.; Gabaldon, A. Modelling of magnetic anisotropy in the finite element method. *COMPEL* **2006**, *25*, 609–615. [CrossRef]
7. Tamaki, T.; Fujisaki, K.; Wajima, K.; Fujiwara, K. Comparison of Magnetic Field Analysis Methods Considering Magnetic Anisotropy. *IEEE Trans. Magn.* **2010**, *46*, 187–190. [CrossRef]
8. Demenko, A.; Nowak, L.; Pietrowski, W. Calculation of magnetization characteristic of a squirrel cage machine using edge element method. *COMPEL* **2004**, *23*, 1110–1118. [CrossRef]
9. Alberti, L.; Bianchi, N. Finite element estimation of induction motor parameters for sensorless applications. *COMPEL* **2012**, *31*, 191–205. [CrossRef]

10. Mazgaj, W.; Szular, Z.; Warzecha, A. Influence of magnetic anisotropy on flux density changes in dynamo steel sheets. *Arch. Electr. Eng.* **2015**, *64*, 81–88. [CrossRef]
11. Warzecha, A.; Mazgaj, W. Identification techniques of functions approximating magnetization characteristics of synchronous machines. *COMPEL* **2013**, *32*, 1267–1277. [CrossRef]
12. Shin, S.; Kim, J.; Lee, S.; Lim, C.; Wiedenbrug, E. Evaluation of the Influence of Rotor Magnetic Anisotropy on Condition Monitoring of Two-Pole Induction Motors. *IEEE Trans. Ind. Appl.* **2015**, *51*, 2896–2904. [CrossRef]
13. Antonio-Daviu, J.A.; Pons-Llinares, J.; Shin, S.; Lee, K.W.; Lee, S.B. Reliable detection of induction motor rotor faults under the influence of rotor core magnetic anisotropy. In Proceedings of the 2015 IEEE 10th International Symposium on Diagnostics for Electrical Machines, Power Electronics and Drives (SDEMPED), Guarda, Portugal, 1–4 September 2015; pp. 14–21. [CrossRef]
14. Henao, H.; Martis, C.; Capolino, G.A. Analytical Approach of the frequency response for the wound rotor induction machine for diagnosis purpose. In Proceedings of the 2005 5th IEEE International Symposium on Diagnostics for Electric Machines, Power Electronics and Drives, Vienna, Austria, 7–9 September 2005. [CrossRef]
15. Maciołek, W.; Sobczyk, T.J. Influence of Magnetic Saturation on Diagnostic Signal of Induction Motor Cage Faults. In Proceedings of the 2007 IEEE International Symposium on Diagnostics for Electric Machines, Power Electronics and Drives, Cracow, Poland, 6–8 September 2007. [CrossRef]
16. Warzecha, A. A frequency domain detection of magnetic core anisotropy of an induction motor. In Proceedings of the 2018 International Symposium on Electrical Machines (SME), Andrychów, Poland, 10–13 June 2018. [CrossRef]